Review

www.the-innovation.org

Recent progress in Chinese fusion research based on superconducting tokamak configuration

Jinxing Zheng,[1] Jinggang Qin,[1] Kun Lu,[1] Min Xu,[2] Xuru Duan,[2] Guosheng Xu,[1] Jiansheng Hu,[1] Xianzu Gong,[1] Qing Zang,[1] Zhihong Liu,[1] Liang Wang,[1] Rui Ding,[1] Jiming Chen,[2] Pengyuan Li,[2] Lei Xue,[2] Lijun Cai,[2] and Yuntao Song[1,*]

*Correspondence: songyt@ipp.ac.cn

Received: October 28, 2021; Accepted: June 8, 2022; Published Online: June 11, 2022; https://doi.org/10.1016/j.xinn.2022.100269

GRAPHICAL ABSTRACT

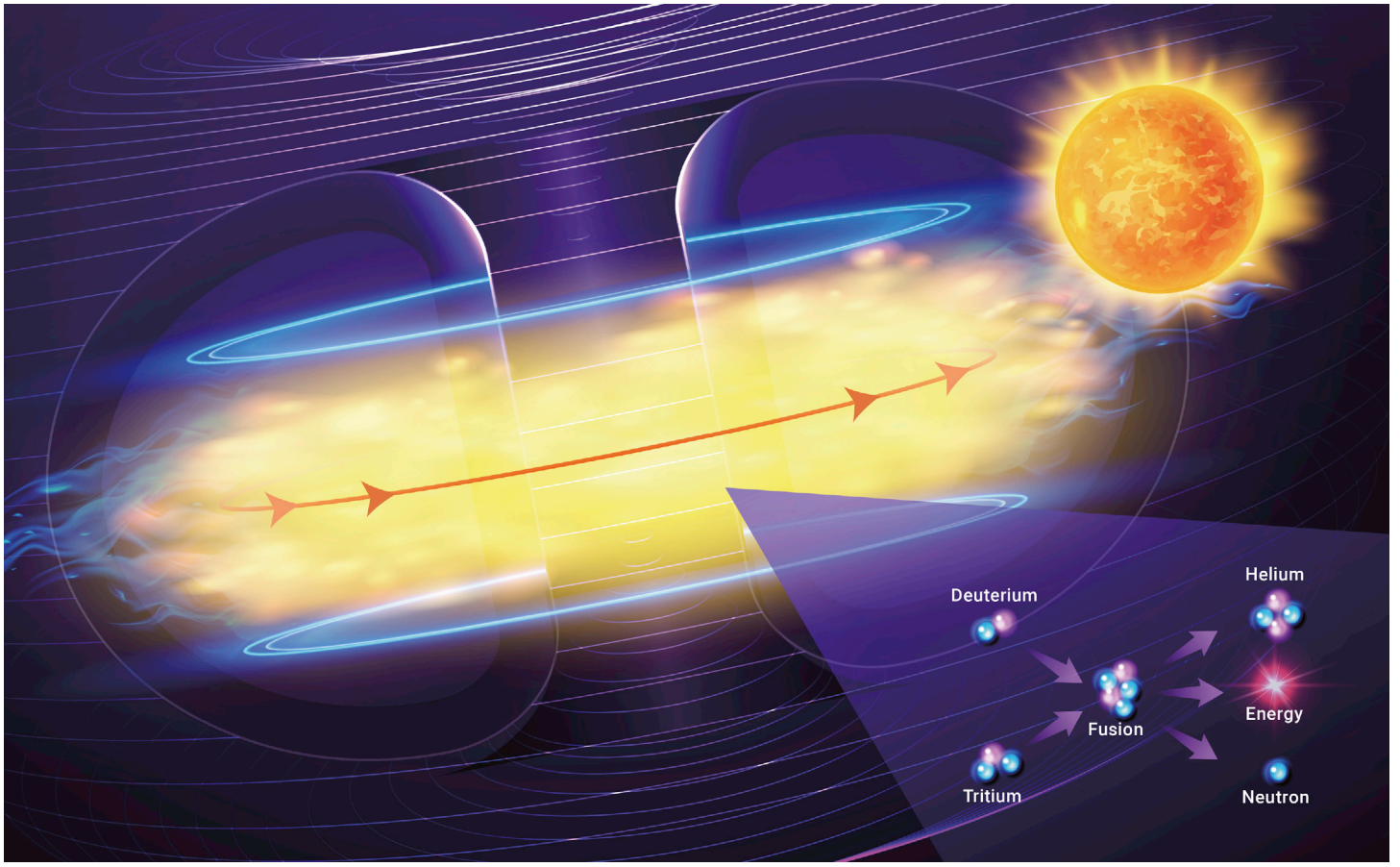

PUBLIC SUMMARY

- Fusion energy is a promising source of clean energy
- Tokamak is the most widely studied magnetic confinement fusion device
- China built the world's first fully superconducting tokamak -EAST
- China is one of the seven members of the ITER project
- CFETR engineering design has been completed, and its R&D is ongoing

Review

Recent progress in Chinese fusion research based on superconducting tokamak configuration

Jinxing Zheng,[1] Jinggang Qin,[1] Kun Lu,[1] Min Xu,[2] Xuru Duan,[2] Guosheng Xu,[1] Jiansheng Hu,[1] Xianzu Gong,[1] Qing Zang,[1] Zhihong Liu,[1] Liang Wang,[1] Rui Ding,[1] Jiming Chen,[2] Pengyuan Li,[2] Lei Xue,[2] Lijun Cai,[2] and Yuntao Song[1,*]

[1]Institute of Plasma Physics, Hefei Institute of Physical Science, Chinese Academy of Sciences, Hefei 230031, China

[2]Southwestern Institute of Physics, Chengdu 610041, China

*Correspondence: songyt@ipp.ac.cn

Received: October 28, 2021; Accepted: June 8, 2022; Published Online: June 11, 2022; https://doi.org/10.1016/j.xinn.2022.100269

Citation: Zheng J., Qin J., Lu K., et al., (2022). Recent progress in Chinese fusion research based on superconducting tokamak configuration. The Innovation **3(4)**, 100269.

Fusion energy is a promising source of clean energy, which could solve energy shortages and environmental pollution. Research into controlled fusion energy has been ongoing for over half a century. China has created a clear roadmap for magnetic confinement fusion development, where superconducting tokamaks will be used in commercial fusion reactors. The Experimental Advanced Superconducting Tokamak (EAST) is the world's first fully superconducting tokamak with upper and lower divertors, which aims at long-pulse, steady-state, H-mode operation, and 101-s H-mode discharge had been achieved. In 2007, China joined the International Thermonuclear Experimental Reactor (ITER) and became one of its seven members. Thirteen procurement packages are undertaken by China, covering superconducting magnets, power supplies, plasma-facing components (PFCs), diagnostics, etc. To bridge the gap between the ITER and fusion demonstration power plants (DEMOs), China is planning to build the Chinese Fusion Engineering Testing Reactor (CFETR) to demonstrate related technologies and physics models. The engineering design of the CFETR was completed in 2020, and Comprehensive Research Facilities for Fusion Technology (CRAFT) are being constructed to explore the key technologies used in the CFETR.

INTRODUCTION

Energy is a crucial driver for development of society. Currently, more than 85% of all energy production is based on traditional fossil fuels such as coal, oil, and natural gas, which are non-renewable energy resources and create pollution.[1] As the world's most populous country, China is facing a critical energy shortage and environmental pollution issues. To achieve sustainable development, there is an urgent need for new sustainable energy sources to meet the fast-growing demand for clean energy. Nuclear fusion is one of the few options that can satisfy the requirements of large-scale sustainable energy generation and global warming mitigation.[2]

The working gases for nuclear fusion reactions are generally hydrogen isotopes D and T. Under certain conditions, deuterium and tritium nuclei can fuse into a heavier helium nucleus, releasing a neutron. The sum of the mass of the produced helium nucleus and a neutron is less than the sum of the mass of the initial deuterium and tritium nuclei. Therefore, based on Einstein's most famous formula, $E = mc^2$, the mass defect during the reaction is converted into a large amount of energy, referred to as fusion energy. Unlike the conditions on the sun, where the fusion reaction takes place because of extremely high pressure (150 billion bar), realization of fusion reactions on earth is extremely difficult because they cannot rely on gravitational confinement as on the sun. Based on theory, fusion ignition can be assessed by the Lawson criterion ($nT\tau_E \geq 5 \times 10^{21}$ keV/m^3; where n, T, and τ_E are the ion density, plasma temperature, and energy confinement time, respectively).[3] From the Lawson criterion, to achieve fusion, a temperature higher than 100 million °C is necessary, which is big challenge from an engineering aspect.

Magnetic field is applied as confinement container to retain hot plasma at a temperature higher than 10 keV in magnetic confinement fusion (MCF) devices. Three types of MCF devices are commonly used: magnetic mirror, stellarator, and tokamak. The magnetic mirror is the simplest device among these, but it has poor confinement ability. The stellarator has good confinement and can achieve steady-state operation with less magnetohydrodynamic (MHD) instabilities and is nearly disruption free.[4] However, the stellarator has a very complex structure and is difficult to manufacture. Tokamaks are the most widely used MCF machines in the world; they have better confinement and are easy to build. In a tokamak, the helical magnetic field is formed by a toroidal field generated by the coils together with a poloidal field generated by the plasma current.[4] Fusion power is positively correlated with the intensity of the magnetic field; thus, to produce a large magnetic field and minimize power consumption, a superconducting tokamak has been proposed.

Based on the energy needs of China, fusion programs are becoming an important and vital component of the Chinese nuclear power program.[5] There are two main fusion research centers in China: the Institute of Plasma Physics, Chinese Academic of Sciences (ASIPP), Hefei, and the Southwestern Institute of Physics (SWIP), Chengdu. In addition, several Chinese universities are actively undertaking fusion research, including Tsinghua University and Huazhong University of Science and Technology. In this paper, the progress of Chinese fusion research is reviewed.

ROADMAP OF CN-MCF DEVELOPMENT

Because of the advantages of tokamaks mentioned above, the Chinese fusion research community has focused on tokamak plasma for several decades. From 1980 to the mid-1990s, several tokamaks with small and medium sizes were developed, such as HT-6B,[6] HT-6M,[7] HL-1,[8] and HL-1M.[9] At that stage, the research effort mainly focused on basic plasma physics and training emerging scientists. In 1994 and 2002, two prominent tokamaks, HT-7 and HL-2A, were built separately at ASIPP and SWIP, based on devices received from Russia (T-7 tokamak) and Germany (ASDEX tokamak), respectively. The HT-7 tokamak made China the fourth country with the ability to develop superconducting tokamaks. Significant progress has been made, marked by the first H-mode plasma in HL-2A[10] and 400-s discharge at an electron temperature of 1 keV in HT-7.[2] These advancements have laid an important foundation for Chinese research into MCFs. To direct research into Chinese MCFs in the short term and longer, consensus has been achieved regarding early application of fusion energy in China; a CN-MCF roadmap is shown in Figure 1.

The short-term targets of CN-MCF research are as follows: (1) establish advanced platforms for plasma physics research in China (Experimental Advanced Superconducting Tokamak [EAST], aiming to accomplish long-pulse H-mode and steady-state operation with modern heating and current drive and diagnostics; HL-2M, aiming to investigate high-performance plasma physics under high auxiliary heating power;[11] and J-TEXT, focused on plasma disruption and plasma turbulence transport);[12] (2) develop key technologies for construction of the International Thermonuclear Experimental Reactor (ITER) and Chinese Fusion Engineering Testing Reactor (CFETR); and (3) designing the CFETR. Construction of the CFETR is expected to be finished in the 2030s. There are two phases planned for CFETR operation. In phase I, the target is to achieve 100–200 MW of fusion power. Steady-state operation and tritium self-sufficiency will be explored in this phase, complementary to ITER Q = 10 operation. Phase II is planned to be completed in the 2040s. The most important issues faced by the fusion demonstration power plant (DEMO) tokamak at a fusion power of 1 GW will be demonstrated in CFETR phase II. The prototype fusion power plant (PFPP) is planned to be built by around 2060, which is the final step of the CN-MCF roadmap toward establishing a commercial fusion power plant.

Currently, the EAST is becoming one of the key tokamaks in the world; it can provide high-performance, long-pulse operation scenarios for future devices, including the ITER, CFETR, and DEMO. The engineering design of the CFETR started in 2017,[13] which is about 10 years earlier than that of the EU-DEMO and Japan-DEMO, whose engineering designs are planned to commence in 2029[14] and 2025,[15] respectively.

The rest of this paper is organized as follows. The section titled as "The EAST project and related activities" covers the main research activities and results of

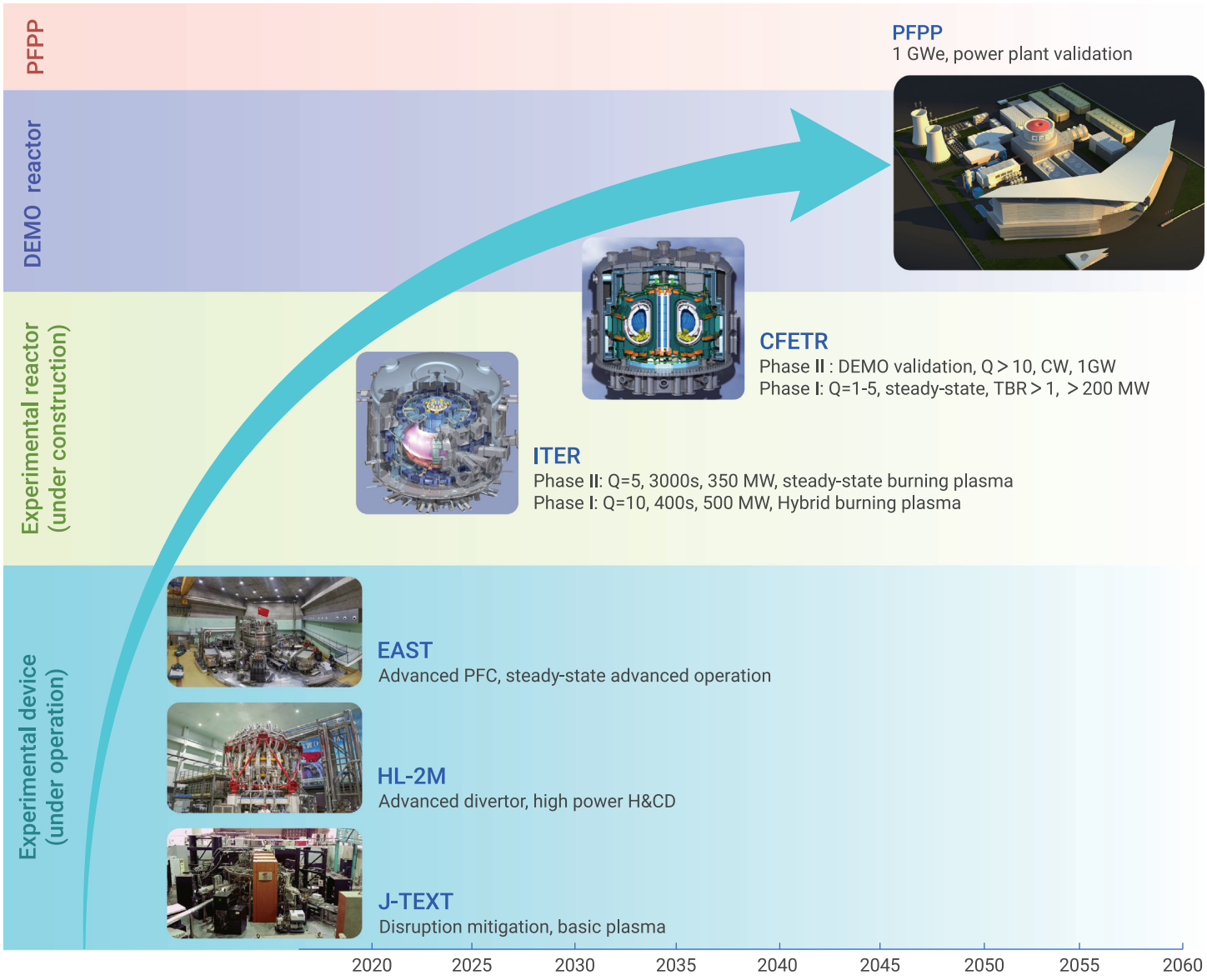

Figure 1. Roadmap of China's MCF development

the past 10 years regarding the engineering progress of the EAST. The progress of ITER activities in China is introduced in the section of "Progress of ITER activities". The section named as "Design and R&D activities of CFETR and DEMO" covers the design and R&D activities of the CFETR and DEMO. The application prospects are presented in the last section.

THE EAST PROJECT AND RELATED ACTIVITIES

The main plasma-related parameters and acronyms that will be used in the following sections are summarized in Table 1.

Overview of EAST

The EAST[16,17] is the world's first fully superconducting tokamak device with advanced divertor configurations and heating scheme similar to that of the ITER; it was built at ASIPP and has run since 2006 (Figure 2A. The main objectives of the EAST are to demonstrate long-pulse divertor operation over 1,000 s and achieve high-performance H-mode operation over hundreds of seconds, addressing key physics and engineering issues for future fusion devices, such as the ITER, CFETR, and DEMO. The major and minor radii of the EAST are R = 1.7–1.9 m and a = 0.4–0.45 m, respectively. The toroidal field and maximum plasma current presently achieved are B_T = 3.5 T and I_p = 1 MA, which will be increased later to 4 T and 1.5 MA, respectively, by reducing the temperature of the superconducting magnets from 4.5 to ~3.8 K. The machine can be operated in lower single null (LSN), double null (DN), and upper single null (USN) divertor configurations with a flexible poloidal field control system and can also periodically switch between LSN, DN, and USN configurations to facilitate long-pulse plasma operation.[18] Changing of the configuration makes it a convenient tool for investigating divertor configuration effects on divertor asymmetry and H-mode access. The DN configuration is currently interesting for DEMO design because it can reduce the heat flux on the divertor and achieve higher confinement.[19]

Since completion of construction and achievement of the first plasma in a limiter configuration with a fully stainless steel wall, its operation and research capability have increased every year through development or upgrade of plasma control, wall conditioning, active cooling of the in-vessel components, heating/current drives, etc. To handle the high heat fluxes during high performance, steady-state, H-mode discharging, all of the EAST plasma-facing components (PFCs) are actively cooled (Figure 2B).

Over the past few years, the EAST has been upgraded with an ITER-like active water-cooling tungsten divertor (Figure 2C) and is capable of handling a power load up to 10 MW/m^2 for long-pulse steady-state operation with high power injection.[20]

New EAST upgrades and current capabilities

The EAST is equipped with several auxiliary heating systems, such as those for lower hybrid current drive (LHCD) systems used in plasma current drives and electron heating (2.45 GHz [4 MW]/4.6 GHz [6 MW] klystron power) (Figure 2D), electron cyclotron resonance heating (ECRH) systems (140 GHz [2 MW] gyrotron

Table 1. Definition of the main plasma-related parameters and acronyms

Item	Definition
I_p	plasma current
q_{95}	safety factor
T_e, T_i	electron temperature, ion temperature of the plasma
n_e	electron density
β_N, β_P	normalized beta, poloidal beta
H_{98}	energy confinement enhanced factor
B_T	toroidal magnetic field,
R, a	plasma major radius, plasma minor radius
V-loop	plasma loop voltage
L-mode, H-mode	low confinement mode, high-confinement mode
E_r	radial electric field
D_α	deuterium Dα line, is a common diagnostic of recycling particles in a tokamak

power), ion cyclotron resonance frequency (ICRF) systems (27–80 MHz [12 MW] generator power), and balanced neutral beam injection (NBI) systems (two co-current and two counter-current NBI sources [80 keV/4 MW]). The augmented heating and current drive (H&CD) capabilities provide sufficient flexibility to assess scenarios for steady-state operation on the EAST.

In addition, nearly 80 modern diagnostics have been developed and implemented on the EAST, which are capable of measuring the dynamics of plasma profiles, instabilities, and plasma-wall interactions during long-pulse operation.[21] All magnetic sensors have been installed in the vacuum chamber as an integral part of the in-vessel components, which can provide sufficient information about machine operation, plasma control, and physics analysis. The radial profiles of key plasma parameters, such as the contents of T_e, n_e, and T_i, along with the rotation, are available during the experiments. Thomson scatter (TS) systems can be used to determine the electron density ne and temperature T_e with a time interval of 20 ms.[22,23] The advanced X-ray imaging crystal spectrometer (XCS), which can be used to record temporally and spatially resolved spectra of helium-like argon ions from multiple sight lines through plasma, is a powerful diagnostic tool for measurement of ion and electron temperature profiles as well as plasma toroidal rotation. [24] A fast-ion D-alpha spectrum (FIDA) has been developed to assess fast-ion behavior and energetic particle-related physics.[25] Particular attention has been paid to plasma core-edge diagnostics, such as lithium beam emission spectroscopy (Li-BES) to obtain edge electron density profiles.[26] An 11-chord, double-pass, radial viewing, and far-infrared laser-based polarimeter-interferometer (POINT) system has routinely operated for diagnosing the plasma current and electron density profiles during plasma discharge.[27]

Based on the hardware mentioned above, an understanding of the high-performance long-pulse operation of the EAST is obtained, facilitating design of next-generation fusion reactors such as the ITER and CFETR.

Steady-state operation of the EAST

H-mode operation is currently envisaged to be the operating mode of the DEMO and future fusion power plants.[28] Achieving steady-state and long-pulse high-performance plasma is an important goal for EAST physics research, which can help to investigate the relevant physics and issues of the future fusion devices. The first H-mode in the EAST was achieved in 2010. In the 2012 campaign, the EAST achieved highly reproducible, world-record, long-pulse, H-mode

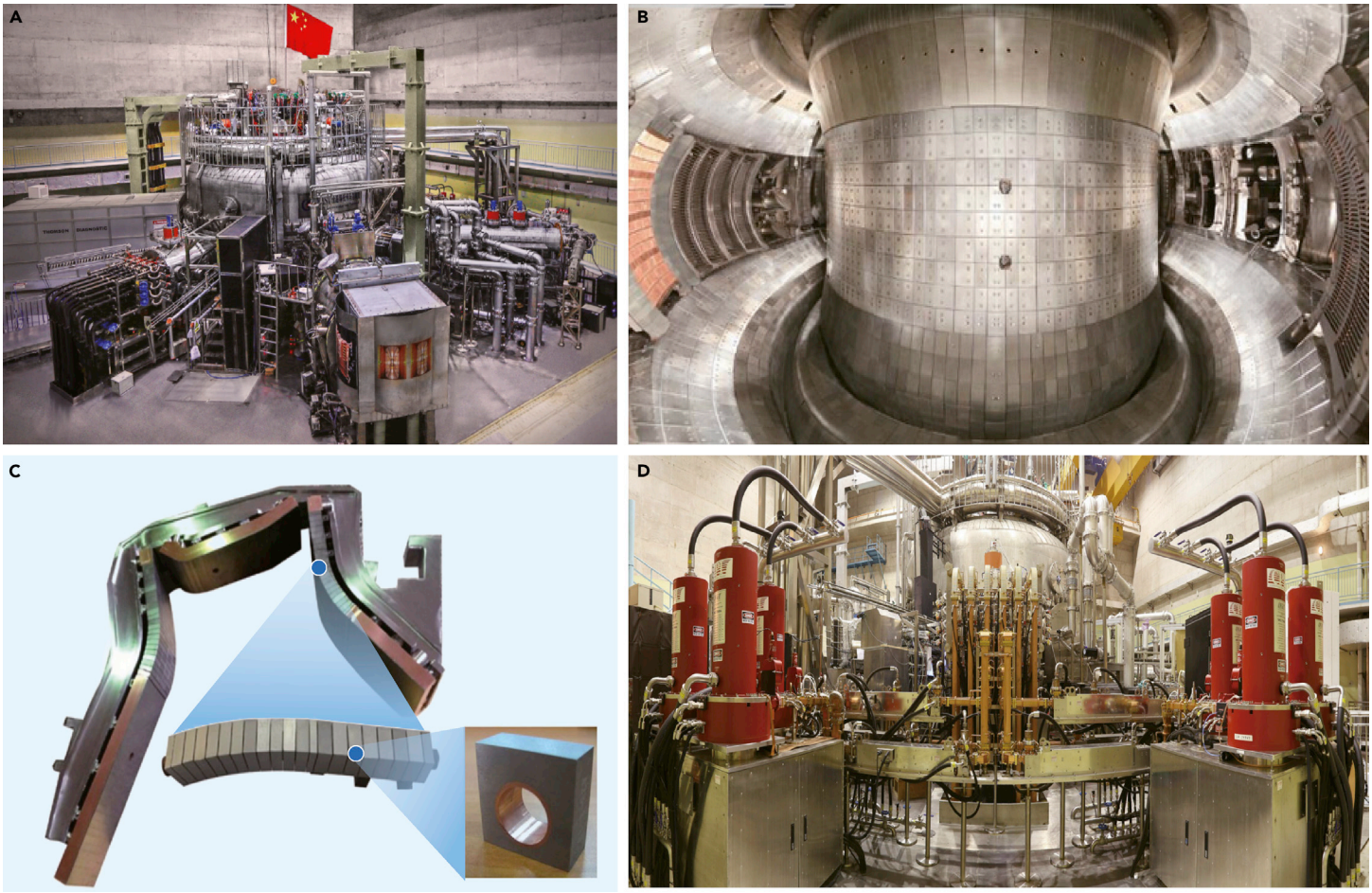

Figure 2. The EAST tokamak (A) Overall view of the EAST from outside. (B) Overall view of the PFCs. (C) One sector of the upper divertor based on ITER-like W monoblocks. (D) Overall view of the LHCD plasma heating system.

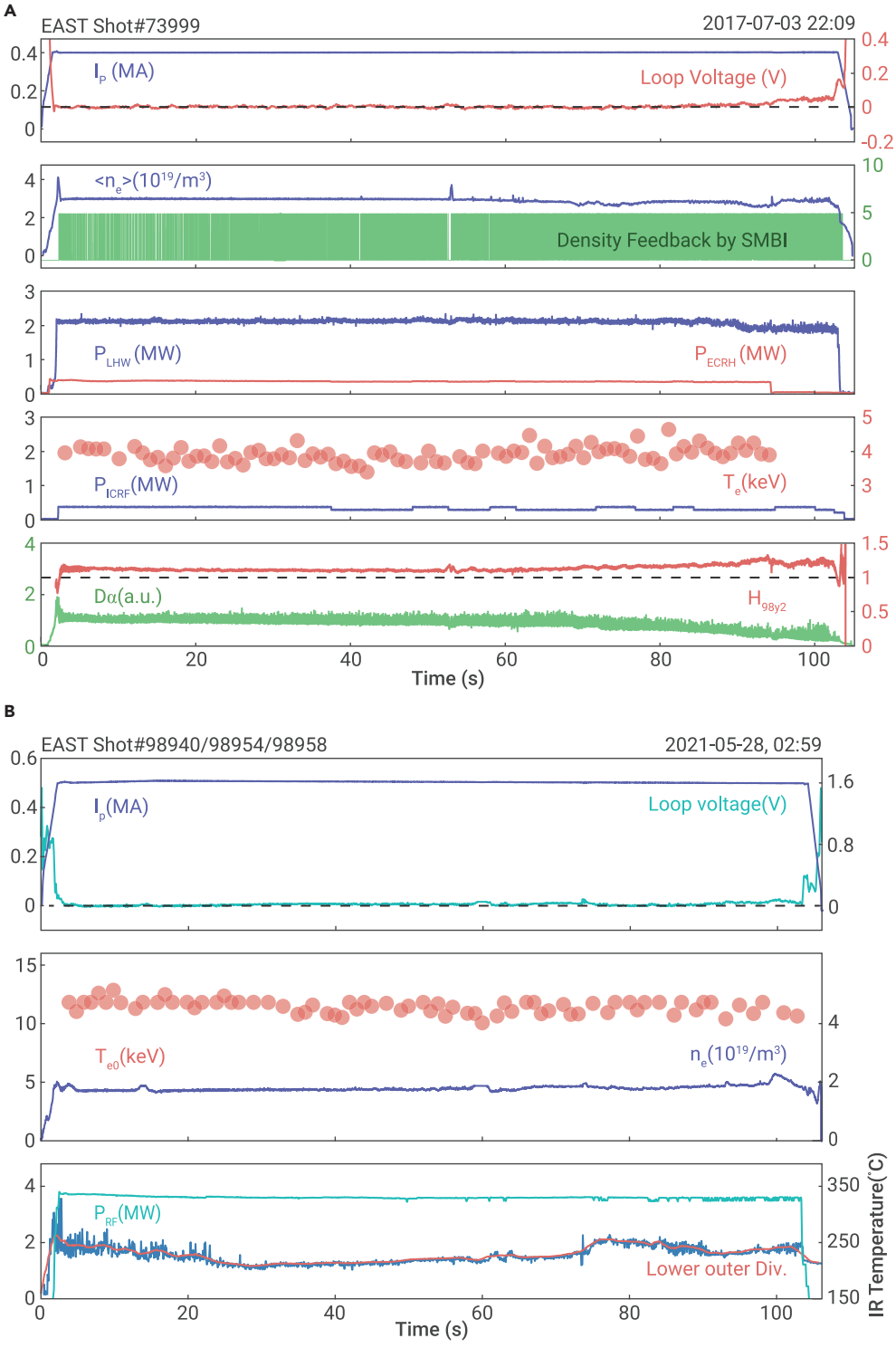

Figure 3. EAST long pulse discharge results (A) 101-s H-mode discharge. (B) 101-s repeatable discharge with a plasma temperature of 120 million °C.[34]

operation of over 30 s[29] and steady-state divertor operation over 400 s with a nearly fully non-inductive current drive.[17]

Since 2015, the EAST has been equipped with all ITER-relevant auxiliary H&CD systems, aiming to provide a suitable platform to address physics and technology-related issues relevant to steady-state, advanced, high-performance, H-mode plasmas.[30–33] A repeatable 100-s-long pulse steady-state scenario with good plasma performance (H_{98}(y2) ~1.1) and heat exhaust with a tungsten divertor was achieved on the EAST in 2017 (Figure 3A). The plasma parameters of 98940, 98954, and 98958 are plasma current Ip = 0.4 MA, normalized poloidal beta (β_P) ~1.2, toroidal magnetic field B_T = 2.5 T, USN with elongation k = 1.6, and safety factor at the 95% normalized poloidal flux surface q_{95} ~6.6.

Development of high β_P scenarios with high bootstrap current fractions during long-pulse H-mode operation—heated by lower hybrid wave (LHW) and ECRH systems—is another key goal of the EAST. Recently, a higher plasma beta ($\beta_P \sim 2.5$ and $\beta_N \sim 1.9$) for a period of 8 s has been achieved when co- and ctr-Ip NBI were applied. In addition, a high β_N scenario has been carried out in the EAST. A typical high β_N plasma discharge has the following parameters: I_P = 400–500 kA, B_T = 1.5–1.6 T, and q_{95} = 3.4–4.4. In this discharge, the plasma density increases to 5.5 ×10^{19}/m^3 (Greenwald factor up to 0.75), and β_N up to 2.1 has been obtained with good plasma confinement (H_{98}(y2) = 1.1). An internal transport barrier (ITB) has often been observed in these high β_N scenario H-mode plasmas after increasing the NBI power. The ITB can be obtained on the EAST with various types of plasma current profiles, including monotonic, central flat (q(0) ~ 1), and reversed shear current profiles. The MHD instabilities associated with these different types of current profiles have been studied. It was found that the fishbone mode (m/n = 1/1) can be beneficial to sustain the central flat (q(0) ~ 1)q profile; therefore, a stable ITB can be obtained. Reverse-sheared Alfvén eigenmodes have been observed in the reverse-sheared plasma with transient ITB formation. The role of the plasma current profile in formation of the ITB must be further investigated, and this operation regimen could be important for development of a hybrid scenario for the ITER and CFETR.[21]

In the 2018 EAST campaign, the first fully non-inductive discharge with a high core electron temperature (Te_0 > 9 keV) was carried out, which is one of the main experimental goals of the EAST. A novel helical m/n = 1/1 (m is the poloidal mode number and n is the toroidal mode number) saturated steady mode was observed in the center of the EAST electron-heating dominant plasma.[35] Analyzing the physics of the high-performance plasma could facilitate further development of this scenario for a longer pulse duration and higher temperature in the core.

Currently, the phase-III upgrade of the EAST has been completed. In the latest EAST campaign, the EAST reached another milestone of achieving plasma at an electron temperature of 120 million °C for 101 s (Figure 3B). In addition, a 1,056-s-long pulse discharge was also obtained.[36] The EAST passed its 100,000th discharge after 15 years of operation, verifying the stability of the EAST. The tokamak is on course to meet its next targets, which are 400-s H-mode operation and 100-s 10-MW operation.

Physics of L-H transition on the EAST

Studying the low-to-high (L-H) confinement transition in toroidal magnetic confinement systems is significant for understanding the physics of fusion energy. In 2014, the EAST completed its phase II upgrade. In addition to an engineering upgrade, significant progress was made in terms of the H-mode physics for long-pulse operation. Although H-mode plasma had been successfully and

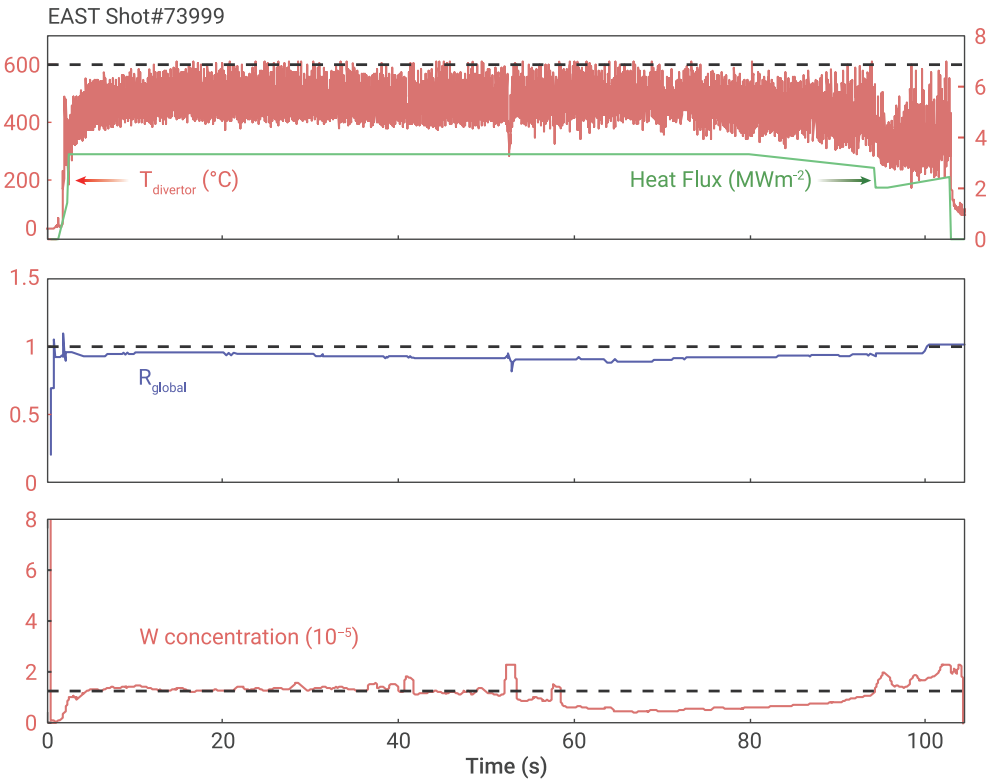

Figure 4. Time evolution of peak divertor target temperature, global recycling, and W concentration in core plasma during the 100-s H-mode in the EAST

reliably obtained on the EAST, the predictions for the H-mode power threshold remained uncertain because the physics of the L-H transition are not yet fully understood.[37] To investigate the mechanism of L-H transition, a long-term physics study was carried out on the EAST. In 2011, a quasiperiodic low-frequency Er oscillation and modulation in edge turbulence—preceding and following the L-H transition—have been observed in the EAST, providing the first evidence of the role of zonal flows in the L-H transition at a marginal input power.[38] In 2016, a new L-H transition model was developed based on the new turbulence suppression mechanism, and rapid transition could occur, spontaneously mediated by a shift in the radial wavenumber spectrum of turbulence without the assistance of zonal flows.[39]

The periodic crash of the pedestal in H-mode plasmas, known as edge-localized mode (ELM),[40] can lead to significant energy loss, production of transient particles, and heat flux on the PFCs. Uncontrolled type I ELM can cause significant damage to the materials of ITER PFCs in H-mode plasmas.[41] Therefore, ELM control is an important issue in tokamak fusion research.

Since 2014, the EAST has been investigating ELM control with the most existing methods, including resonant magnetic perturbations (RMPs),[41] pellet pacing,[42] supersonic molecular beam injection,[43] LHWs,[44] and Li pellet injection,[45] allowing it to achieve long-pulse steady-state operation. The nonlinear transition from mitigation to suppression of the ELMs by using RMPs was first observed in the EAST in 2016.[46] Strong mitigation of ELMs has been observed in the EAST when LHWs are applied to H-mode plasma with ion cyclotron resonant heating.[47] An 18-s-long-pulse H-mode with a record ELM-free period was achieved in the EAST through real-time injection of a Li aerosol into the edge plasma, which actively suppressed ELM formation and prevented impurity accumulation.[48] Evidence of a nonlinear transition from mitigation to suppression of the ELM by using n = 1 and 2 RMPs was observed in the EAST in 2016.[46] This is the first demonstration of ELM suppression with RMPs in slowly rotating plasma with dominant radio frequency wave heating. A reproducible stationary, high-confinement, small grassy ELM regimen has been demonstrated in the EAST.[49] This regimen is proposed as the primary ELM mitigation solution for the CFETR and offers a highly promising operational scenario for future steady-state fusion beyond the ITER.

To verify the theory that Er × B shear can affect the magnitude and evolution of the cross phase of the velocity and pressure fluctuations in the peeling-ballooning mode-driven heat flux, an alternating Er × B flow shear discharge was performed using the specific co-NBI and ctr-NBI systems in the EAST. The new results[50] show that the increased Er × B flow shear can significantly mitigate the ELM or even totally suppress the ELM when the shear is large enough. Simulations with BOUT++ support the observations made in the EAST, which indicates that the increased Er × B can reduce the linear growth rate of the ballooning mode and shorten its growth time (phase coherence time [PCT]). The enhanced nonlinear interactions shorten the PCT of the ballooning mode, which is validated by a bispectrum study on the EAST. All of these analyses studies suggest a new method to control the ELM.

Power and particle exhaust investigation in the EAST

Active control of the excessively high heat and particle fluxes in the divertor target plates is crucial for steady-state operation of tokamaks. A series of experiments has been carried out systematically to investigate this critical issue and relieve the plasma-wall interactions in the superconducting EAST, not only contributing to the long-pulse operation of the EAST but also providing a physical understanding of and potential techniques for next-generation devices like the ITER and CFETR.

Since the beginning of its operation, the EAST has made significant contributions to the basic physical understanding of fusion and developed new control techniques for divertor/PWI long-pulse operation, including (1) steady-state heat flux control, (2) fueling particle exhaust, and (3) impurity screening, which have been successfully applied to achieve high-confinement (H-mode) plasma for over 100 s[21,51] by making full use of the active water-cooling ITER-like tungsten divertor. Many heat and particle flux control approaches have been developed and tested on the EAST, such as power footprint broadening and 3D deposition;[18,29,47] active heat load control,[52] advanced plasma equilibrium development, such as the quasi-snowflake divertor configuration; divertor particle exhaust optimization; recycling; and tungsten souring control. The upper divertor of the EAST was upgraded from graphite to active water-cooling ITER-like tungsten in 2014, leading to an enhanced heat removal capability.

Recently, active control of detachment or radiation compatible with core plasma performance has advanced significantly,[53–55] with a series of active feedback control modules successfully developed and implemented. These modules have excellent compatibility with high core plasma performance, which has also been demonstrated on Doublet III D (DIII-D) in 2019.[56] In terms of the particle exhaust, including fueling and impurity particles in addition to wall conditioning and impurity source control, the efficiency of the particle flux exhaust is optimized by making full use of the divertor closure and the plasma drifts in the scrape-off layer and divertor volume. For wall conditioning, many advanced methods have been developed and employed in the EAST, including first wall baking, direct-current glow discharge cleaning (DC-GDC), high-frequency GDC (HF-GDC), ICRF discharge cleaning (ICRF-DC), silicon coating (SiD4), lithium coating, and real-time lithium powder injection (LPI) during plasma operation. Long-term wall conditioning is typically employed in this phase to remove low-Z impurities, such as hydrogen, oxygen, nitrogen, and water. Usually, high-temperature baking of the first wall, up to 180°C–200°C, is used, along with DC-GDC using helium and deuterium as the working gases.

These advances in heat and particle exhaust techniques have contributed to a series of EAST achievements, including H-mode operation for over 100 s.[57] By employing the water-cooling ITER-like upper W divertor, along with physics control and optimization approaches for divertor heat and particle exhaust, the EAST has achieved a record long-pulse H-mode operation of over 100 s in the USN configuration; the peak divertor target temperature, global recycling,

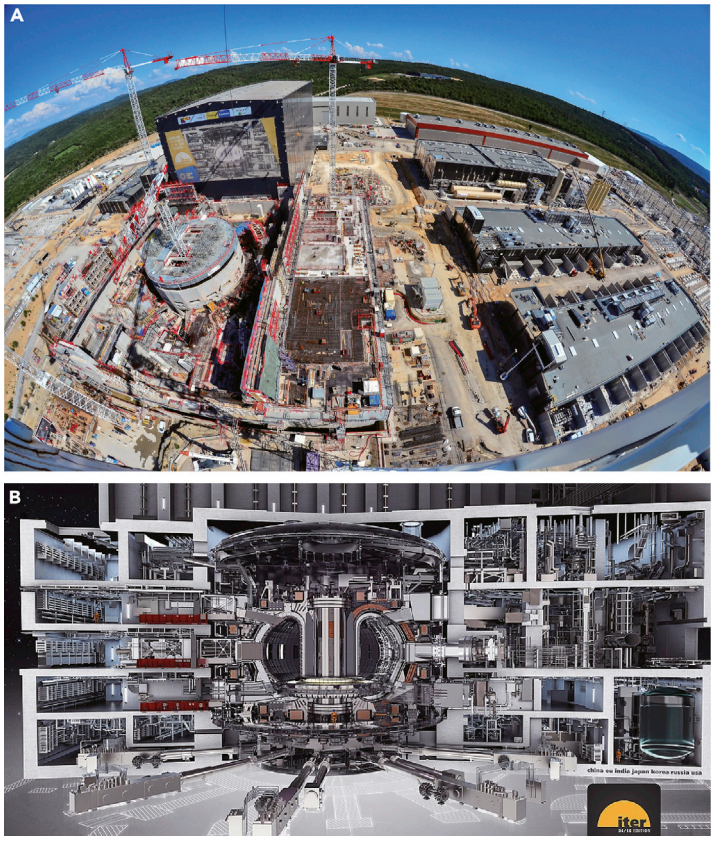

Figure 5. The progress of ITER project (A) The recent ITER assembly site. (B) An overall view of the ITER machine.[62]

W concentration, and core confinement performance are shown in Figure 4. This steady-state scenario was characterized by a fully non-inductive current drive and high-frequency small-amplitude ELMs, which verified the stable control capability of heat and particle exhausts using the ITER-like tungsten divertor at a timescale of 100 s. When the long-pulse discharge reaches wall thermal and particle equilibria, the steady-state peak heat flux on the divertor plates is maintained at ~3.3 MW/m^2 and the particle exhaust rate at ~6.6×10^{20} D/s. As can be seen clearly, the target temperature was maintained below 600°C, the global recycling coefficient was about 0.88 in constant, and the core W concentration was below 2 × 10^{-5}.[58]

More importantly, the energy confinement enhanced factor, H_{98}, during the entire period of discharge, is larger than that of the ITER baseline scenario. The upgrade of the lower advanced tungsten divertor was completed in April 2021, along with the associated divertor diagnostic systems. With these upgraded capabilities, the EAST has become a full-metal wall tokamak, aiming to achieve high-performance long-pulse plasma operation up to 1,000 s. These approaches provide important experimental information regarding divertor-edge-core integration for steady-state operation of future fusion devices.

PROGRESS OF ITER ACTIVITIES

ITER, the world's largest tokamak, is being built to verify the feasibility of fusion as a source of carbon-free energy. It will become the first fusion device to produce a net-positive amount of energy. After construction of the ITER, an experimental campaign will be carried out to advance fusion science and pave the way for future fusion power plants. The primary goal of ITER is to demonstrate steady-state operation of DT plasma producing 500 MW of fusion power for a duration of 300–500 s with a Q factor of at least 10.[59,60] The first ITER plasma production is scheduled for 2025,[61] and assembly of the ITER machine is proceeding steadily (Figures 5A and 5B). There are seven members in the ITER project: China, the European Union, India, Japan, Korea, Russia, and the United States, with the ITER Organization (IO) headquartered in Cadarache, France.

As one of the seven ITER members who joined in 2007, China takes part in the entire process of the ITER project, including design, construction, and operation. In 2008, China signed the first procurement package with the IO, and in the following 5 years, another 13 procurement packages were signed. China is involved in some key components of the ITER machine, including the large-scale superconducting magnet system, the large-scale power supply system, the blanket system, and the diagnostic system. There are two main suppliers for the ITER China Domestic Agency (CNDA): ASIPP and SWIP (two main fusion research centers in China).

Superconducting magnet system

The procurement packages related to ITER superconducting magnet systems include manufacturing of the toroidal field (TF) (7.51%), poloidal field (PF) (65.15%), feeder and correction coil (CC; which was developed to reduce the range of magnetic error fields because of imperfections in the location and geometry of the other coils) (100%) superconductors, ITER CC coils, ITER feeders, and ITER magnet supports. In addition, based on its mega-magnet manufacturing capability, ASIPP won the bid to manufacture the ITER PF6 coil, which was originally a procurement package for the European Union. The ITER TF and PF superconducting conductors, supplied by China, are in cable-in-conduit conductors (CICCs) (Figure 6A), comprising Cr-plated Nb_3Sn (0.82 mm in diameter) and Ni-plated NbTi (0.73 mm in diameter) superconducting strands, respectively. The superconducting strands were supplied by Western Superconducting Technologies (WST; China). All types of superconductors produced by China were qualified by ITER through testing in the SupraLeiterTest Anlage (SULTAN) facility in Switzerland. Assessment of the superconductor's current sharing temperature (Tcs) was one of the most important reasons for conducting the SULTAN test, and the acceptance criterion was 5.8 K[63] Because Nb_3Sn is brittle and strain sensitive, mechanical fatigue on the strands caused by electromagnetic (EM) cyclic loads significantly affects the performance of the superconductor; therefore, the degradation of the Tcs with cyclic EM loading was also assessed in the SULTAN test. The CICC TF conductor sample provided by China shows much higher Tcs values than the design limit, even after 1,000 EM cycles (with a conductor operating current of 68 kA and background magnetic field of 11.8 T). ITER TF conductor procurement was completed in 2015 and was an important milestone for China's participation in ITER. Successful completion of the ITER TF conductor with high quality confirms that China has a high capability of large-scale superconductor development and industrialized production.

In September 2020, ASIPP completed its manufacturing of six bottom CCs (BCC), which are the first batch of CCs delivered to ITER. Nearly 100 people were involved in production of the PF6 coil, which weighs 400 t, measures 10 m in diameter, and has a profile accuracy of ±1.5 mm. The NbTi superconductor used for winding the coil stretches up to 13.5 km. After 6 years of collaborative work between the Chinese and European teams, the first PF coil (PF6) was completed in Hefei, China, in September 2019 (Figure 6B). During the IO acceptance test, the maximum leakage current of the PF6 coil in the Paschen test was found to be less than 4.0 μA (the ITER requirement is less than 20 μA), and the total leakage of the coil was two orders of magnitude lower than required. This project sets a good precedent for collaboration between China and Europe in building a new mode of international fusion collaboration.

ITER feeders are components that supply helium, electrical power, and instrumentation cables to the ITER magnets located in the ITER cryostat.[64] ASIPP is responsible for all of the manufacturing of ITER feeders. In August 2017, the first ITER feeder (PF4 Feeder) was completed in China (Figure 6C), arrived in Cadarche 2 months later, and became the first completed ITER magnet component. Within the ITER Feeder project, the ASIPP team designed key technologies related to development of the high-temperature superconductor (HTS) current leads, which are critical components for the feeder system. 60 HTS current leads with a total nominal current capacity of 2.64 MA will be supplied by ASIPP to the ITER. The insulation voltage of the 68 kA TF HTS current leads is 30 kV, and they have a minimum loss-of-flow accident (LOFA) time of 400 s. The joint resistance of the cartridge high-current-carrying and low-loss joint for the feeders has been minimized to 0.2 nΩ, which can significantly mitigate risks and prevent harmful incidents during ITER operation. Feeder assembly began in the ITER tokamak hall, where the tokamak assembly contract (TAC) is being undertaken by the Chinese consortium.

Figure 6. Progress of ITER activities in China (A) ITER CICC conductors. (B) ITER PF6 coil. (C) ITER feeder. (D) ITER AC/DC converter system. (E) ITER TFGSs. (F) ITER magnet support site assembly.

AC/DC converter of ITER superconducting magnets

ITER AC/DC convertor procurement is the biggest ITER procurement package for China. The convertor power system is an important sub-system for the ITER tokamak; it provides a controllable DC voltage for the superconducting coil. During the ITER AC/DC convertor construction phase, the world's first integrated four-quadrant converter prototype with a non-cophase-counter-parallel connection structure and China's highest-power electrical equipment test platform were developed at ASIPP. During the prototype test, the DC disconnector and external bypass could withstand a short-circuit current of 350 kA, and the DC reactor could withstand a short-circuit current of 175 kA without mechanical damage.[65] In 2015, significant advancements were made in terms of ITER power supply development; five sets of ITER AC/DC converter systems were completed for delivery to the ITER site in France (Figure 6D).

ITER magnet supports

Magnet supports (MS), one of the components to sustain all of the superconducting magnets of the ITER, consists of 18 sets of TF gravity supports (TFGS), 108 sets of PF coil supports (PFCSs) and 6 sets of CC supports (CCSs). MSs not only bear the overall magnet system of more than 10,000 t but also have to be strong enough to sustain unprecedented large loads, such as EM loads, thermal loads, and possible seismic loads during the fusion process. The MS procurement package is fully

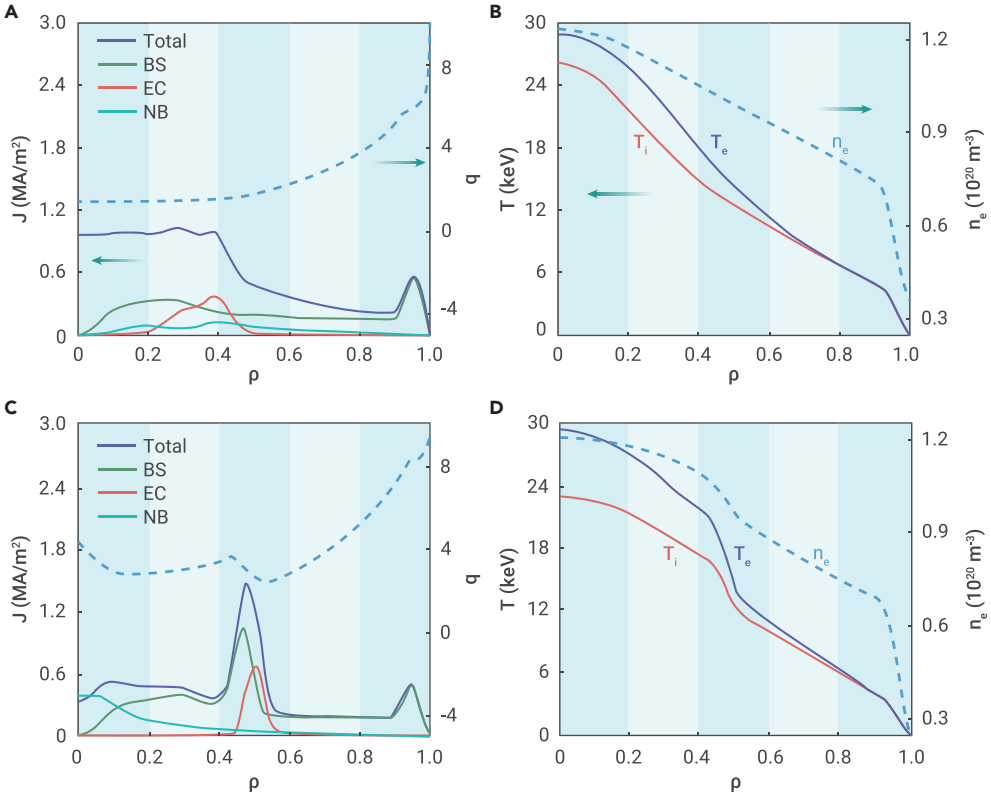

Figure 7. Results of the CFETR integrated modeling
(A) Current profiles for the hybrid scenario. (B) Temperature and density profiles for the hybrid scenario. (C) Current profiles for the steady-state scenario. (D) Temperature and density profiles for the steady-state scenario.

undertaken by SWIP, who shall complete all materials qualification, prototype component fabrication, tests, and series production. Under the joint efforts of SWIP and its suppliers, some technical breakthroughs have been achieved during the past years in terms of high-precision assembly of GS, manufacturing innovation by forging plus wire cutting for the PFCS U-shaped clamps, etc. In June 2018, completion of fabrication and initiation of delivery was announced for the first batch of MS products (Figure 6E). To date, 22 batches of supports, which in total account for 70% of MS products, have been delivered to related receiving parties, including the IO, F4E, JA DA, and RF DA. As one of the most vital structural safety components for the ITER tokomak device, MSs are also some of the first basic units installed at the ITER site in France. So far, all GS, PFCS5, PFCS2, and PFCS6 devices have been installed or pre-installed on related interfaces at the ITER site (Figure 6F).

ITER shielding blanket components

The procurements include ITER enhanced heat flux (EHF) first wall (FW) panels (12%) and shielding blocks (50%). One FW panel consists of a stainless steel central beam (CB) and 40 plasma-facing fingers with pure beryllium tiles, a CuCrZr alloy heat sink, and 316L(N) steel back plate bonded together by hot isostatic pressing technology. After successfully passing the high heat flux test of the full-scale fingers for a semi-prototype without any damage in 2016,[66] the FW procurement arrangement (PA) was signed. After a 2-year effort, the EHF FW design was updated by changing the finger-to-CB welding assembly to a mechanical assembly with an external pipe connection, which mitigates a lot of its operational leak risk by largely reducing the number of welds and improving volumetric nondestructive test accessibility. Now it is in the process qualification phase to manufacture a full-scale prototype. 38 fingers and a CB have been manufactured. The final assembly will be completed in 2022.

The PA for manufacturing the shielding blocks was signed in 2014. In 2018, the full-scale prototype was manufactured and successfully tested in a self-made hot helium leak test facility it was the first one that could meet ITER requirements for shielding block leak testing. Now more than 40 shielding blocks have been completed their final factory tests (FAT), and total progress of the manufacturing is about 39%. The hot helium leak test of the component at 250°C and 4 MPa pressure on the inner cooling surfaces have been fully developed[67] and verified by the series FATs.

An ISO document for this test has been agreed on in 2021 and is in the phase of draft international standard (DIS).

Significance of the ITER activities

Over the past 10 years, China has completed delivery of some key components for the ITER with exemplary characteristics. First, the performance of the TF conductor sample (TFCN1) achieved a world-record Tcs of 6.9 K.[63] Second, the world's highest HTS current lead, at 90 kA, was obtained at ASIPP. China also perfected key technologies for industrial production of Nb_3Sn and NbTi superconducting strands, development of high-temperature superconducting current leads, and hot isostatic pressing of Be/Cu joints. Many large-scale test platforms were developed, providing significant support for R&D of ITER components. The combination of engineering technologies proposed has also been widely applied in civilian industries, such as those involving superconduction, cryogenics, radio frequencies, and functional materials. A professional fusion research team with international vision was established in China, which is very important for the next step in fusion research: design and construction of a Chinese fusion reactor.

DESIGN AND R&D ACTIVITIES OF THE CFETR AND DEMO

CFETR activities

For confined magnetic fusion, the most significant challenge is proving the feasibility of achieving fusion at the power-plant scale. The ITER is already a large-scale machine in comparison with existing tokamak machines. However, it is still experimental and suffers from several engineering issues relevant to commercial fusion power plants. To bridge the gap between the current experimental fusion machines and future fusion power plants, DEMOs are planned to be designed and constructed in some countries.[68,69] As an important part of the roadmap of achieving fusion electricity, the main goals of DEMO construction are as follows: steady-state operation and power output at the power-plant scale and reliable maintenance through use of remote handling tools and tritium, fulfilling self-sufficiency requirements. Significant progress is still needed in terms of reaching DEMO from ITER; therefore, after intensive discussions, China decided to build the CFETR.

The primary goals of the CFETR project are to achieve a fusion energy production of 200–1000 MW and generate steady-state burning plasma with a duty time of about 50%.[70] It aims to realize tritium self-breeding with a tritium breeding ratio (TBR) of 1.0 or higher and to research high-performance materials with good neutron and thermal resistance.

CFETR physics design. The physics design of CFETR mainly focuses on development of the operating scenarios and their optimization with respect to physics and engineering constraints. The feasibility of the fusion power goal of CFETR has been verified. First, reference plasma parameters for hybrid scenarios and steady-state scenarios have been proposed based on calculations using the 0-D system code GASC,[71] and, subsequently, systematic studies using PROCESS[72] showed that there was a reasonable number of feasible operating scenarios for a CFETR with a high fusion power.[70,73] Two-dimensional free boundary equilibrium calculations were then performed to design the plasma shape, which showed that the conventional single null divertor (SND) configuration could be sustained by the PF coils.[74] Compatibility of this SND configuration, along with the power exhaust requirement, was demonstrated through SOLPS simulations.[75] In these simulations, partial detachments for inner and outer

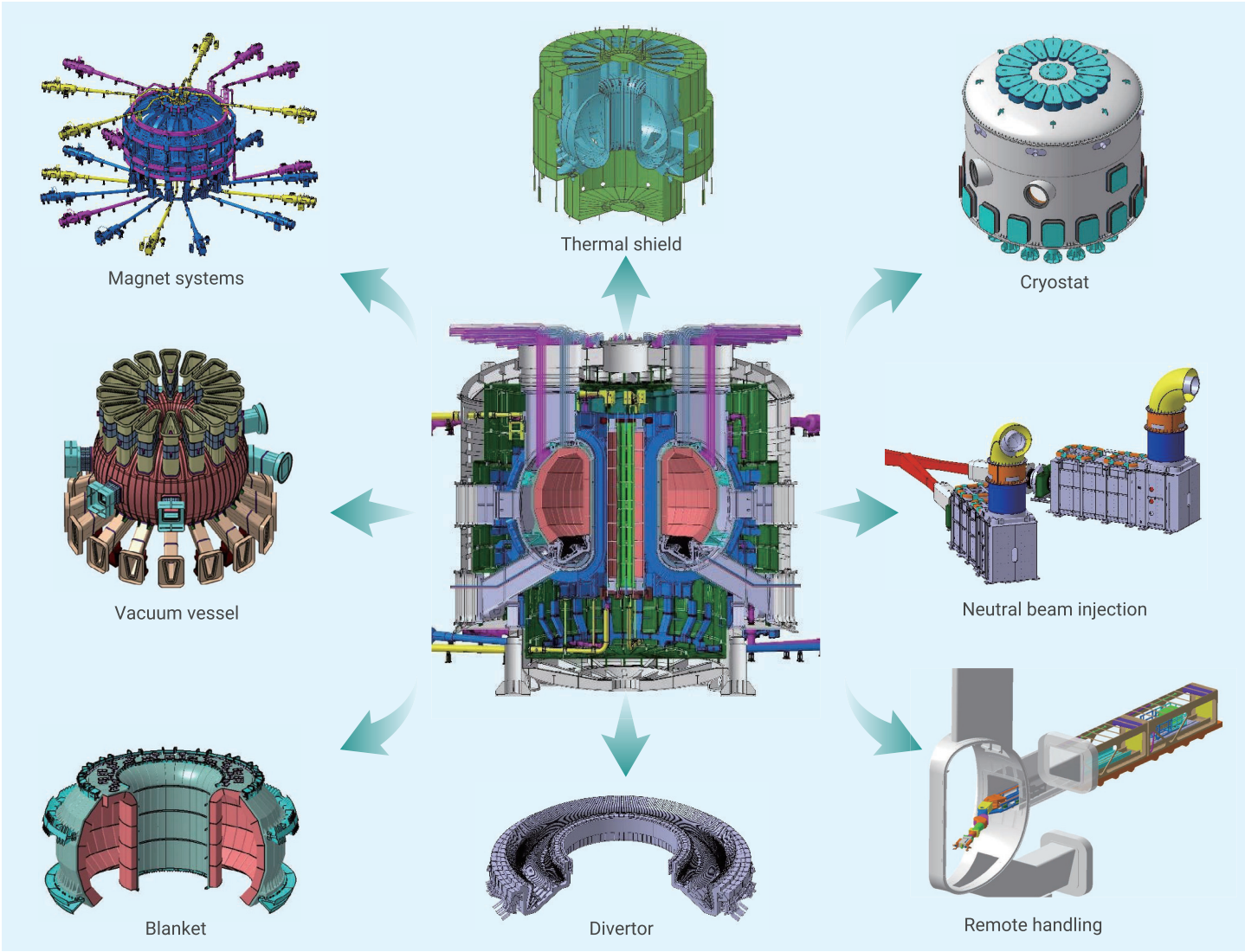

Figure 8. Engineering design of the CFETR

divertor targets were achieved through seeding with neon and deuterium, and the peak heat load was lower than 3 MW/m^2.

The profiles of temperature, density, and current were modeled through integrated modeling with self-consistent core-pedestal coupling.[76] The pedestal profile was modeled using the EPED-1 code,[77] following the constraints caused by stability of the coupled peeling-ballooning (P-B) mode and kinetic ballooning mode (KBM).[11] The plasma transport in the core was a result of the combination of turbulent transport, calculated by the TGLF code,[78] and neoclassic transport, calculated by the *NEO* code.[79] By optimizing the pedestal parameters and current drives, a baseline case for the hybrid scenario with a fusion power of ~1 GW was obtained by combining 30 MW NBI and 50 MW electron cyclotron waves.[80] The confinement (H_{98y2} = 1.14) and normalized beta (~2.3) were moderate in comparison with those in existing tokamak experiments, which verifies the feasibility of obtaining such performance in future experiments. Figure 7 shows the profiles obtained through integrated modeling. The pedestal parameters for the baseline case were compatible with the grassy ELMy condition, according to nonlinear BOUT++ simulations.[81] Based on these modeling cases, with self-consistent calculations for the pedestal parameters and plasma transport in the core, the tritium burnup fraction for the hybrid scenario was modeled by the core-SOL coupling COREDIV code,[82] considering the pellet fueling deep into the core and recycling of fuels and impurities at the edges.[83] The model showed that the burnup fraction could be larger than 3% if the pellet could penetrate deeper than $r/a < 0.8$.

Integrated modeling was also used to explore steady-state scenarios with 1 GW of fusion power. Recent modeling has shown that the combination of a 55-MW electron cyclotron current drive and the bootstrap current could be used to sustain a magnetic shear reversal at ρ = 0.5. The peak of the bootstrap current profile was aligned with the shear reversal because ITBs were formed in the density and temperature profiles, as shown in Figure 7D. The confinement factor (H_{98y2} = 1.33) was high, but it was still lower than the record in the DIII-D high β_P experiments with a similar q profile. The normalized beta reached 2.97, which was still lower than the no-wall limit (~3.0) for ideal MHD modes.[84] Similar analysis results were obtained by using another integrated modeling code, CRONOS. Consequences triggered by extreme events (e.g., electro-magnetic loads during vertical displacement events [VDEs]) were also assessed and were addressed by the following engineering design.

CFETR engineering design. The conceptual design of the CFETR machine began in 2011, comprising two distinct periods. Before 2015, it was designed as a small machine with major and minor radii of 5.7 and 1.6 m, respectively, and B_T of 4–5 T.[85] In the second period, after 2015, the CFETR machine became larger, with major and minor radii of 6.6 and 1.8 m, respectively, and B_T of 6–7 T. In this larger design, the CFETR aimed to achieve 1 GW of fusion power.[70] To fulfill the CFETR project targets, in 2017, a new version of the CFETR key parameters was put forward based on previous engineering and physics research. The plasma major and minor radii increased again to 7.2 and 2.2 m, respectively, and the new B_T was 6.5 T with an I_p of 14 MA.

The engineering design of the CFETR began in 2017. There are eight main tasks associated with all subsystems of the machine, remote handling system, standardization, and design management. Currently, the engineering design has been completed (Figure 8). The CFETR superconducting magnets include the PF coils, TF coils, and central solenoid (CS) coils, all of which are designed

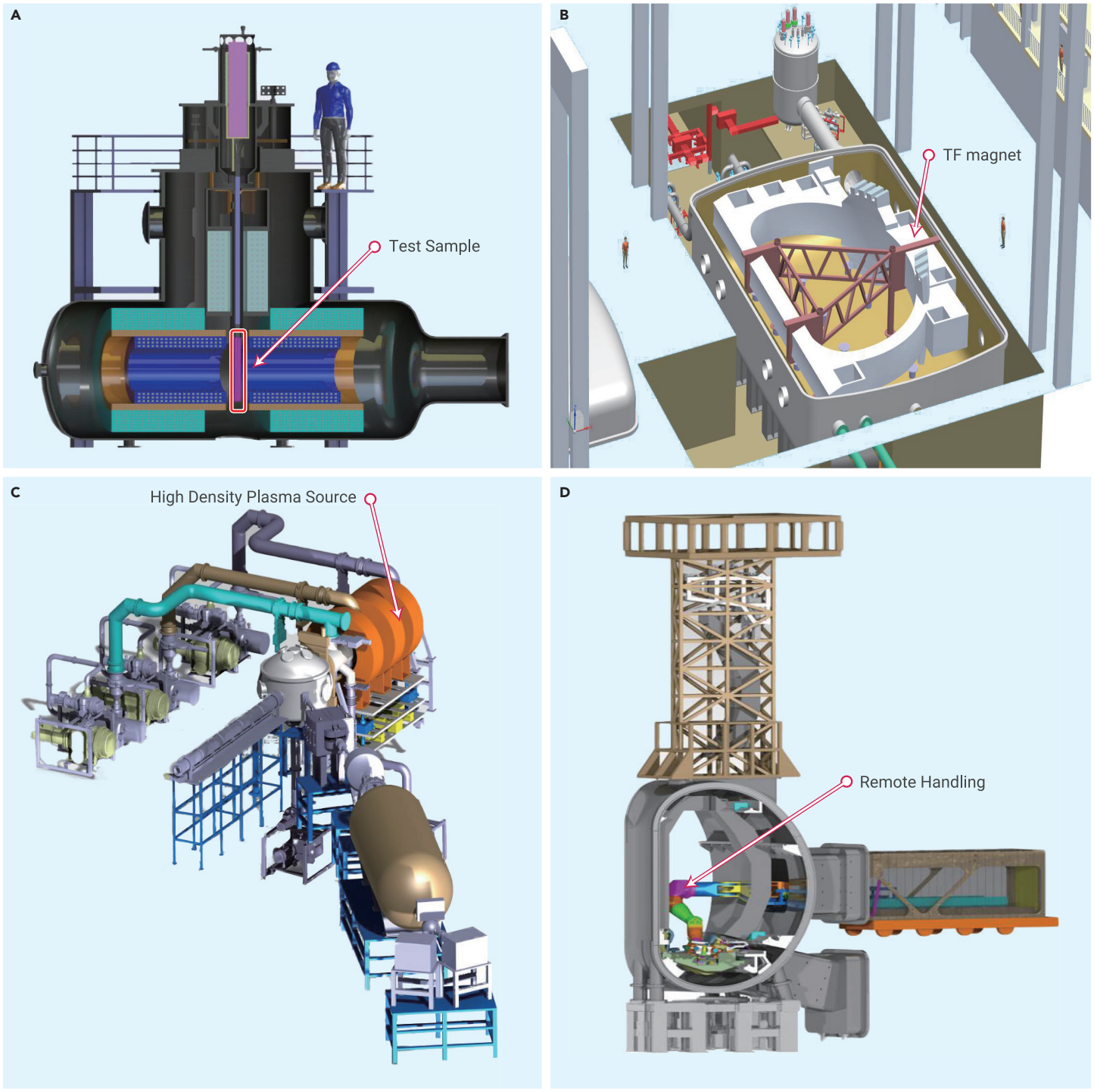

Figure 9. CRAFT system design (A) Conductor testing sub-system. (B) Magnet testing sub-system. (C) Linear plasma testing sub-system. (D) 1/8 VV integration sub-system.

based on CICC superconductors. According to the working position and the differences in the mechanical loads, three kinds of CICCs are applied on 16 identical D-shaped TF coils. In the high-field region (the magnetic field reaches 14.7 T), the high-performance Nb_3Sn CICC is used; in the middle-field region (with a peak field of 11.1 T), the ITER-like Nb_3Sn CICC is used; and in the low-field region (with a peak field of 6.6 T), the NbTi CICC is used. The CS magnet comprises a stack of eight circular coils that are wound with high-Jc Nb_3Sn CICCs. There are seven PF coils designed for the CFETR, where Nb_3Sn is selected for PF1 and PF7 manufacturing and NbTi for the other PF coils. A vacuum vessel (VV) system was designed with an interior volume of 5,072 m^3. Two concepts for the blanket have been designed in parallel: a helium-cooled ceramic breeder (HCCB) blanket and a water-cooled ceramic breeder (WCCB) blanket. For the HCCB, 8-MPa helium gas with an inlet temperature of 300°C is used as the coolant, and 15.5-MPa pressurized water with an inlet temperature of 285°C is utilized as the coolant for the WCCB blanket. For the divertor, two concepts were designed: a helium-cooled divertor and a water-cooled divertor. A steady-state heat flux of 20 MW/m^2 should be safely handled by the CFETR divertor. Being a real nuclear fusion device, the maintenance of the in-vessel components needs to be carried out by various remote handling (RH) systems. The main types of RH systems include the cask and lifting system, the blanket RH system, and the divertor RH system. They will be applied during the maintenance procedures for the blanket and divertor, such as lifting, radial transporting, docking, and fastening.

CFETR R&D activities and future plans. To determine the feasibility of achieving the design parameters for the critical components and to develop

more advanced key technologies for their manufacture, intensive R&D activities have been carried out over the past few years. These R&D activities focus on the magnets, VVs, heating systems, and blankets. A CS model coil, formed using a high-$JcNb_3S_n$ CICC, was developed at ASIPP in 2020. A 1/8 sector real-size VV mock-up is being developed to validate the narrow-gap welding, cutting, and non-destructive testing technologies. Currently, one 1/16 sector of the CFETR VV prototype has been fabricated. The cooling design and bonding technologies of the CFETR blanket have also been developed and tested.

Over the past decade, the conceptual and engineering design of the CFETR has progressed steadily. After the conceptual design phase, the preliminary design of the CFETR machine was completed. Alongside the engineering design, detailed design of the subsystems and their integration were accomplished. R&D activities for CFETR critical components are currently ongoing. Over the next few years, more R&D work will be carried out to validate the key technologies of all subsystems, particularly in the fields of plasma-facing materials, high-temperature superconducting materials, and large heating power systems. To better understand the physics, impurity control, disruption avoidance, vertical instability control, and type IELM control need to be investigated.

CRAFT activities

To understand the key technologies necessary for future fusion reactors, a new facility has commenced construction in 2019, which will last about 6 years. The facility is the Comprehensive Research Facility for Fusion Technology (CRAFT), which falls under the guidelines found in the 13th Five-Year Plan of the Chinese government. For CRAFT construction, the technologies investigated in the ITER project will be used, but several technologies still need to be developed. When completed, it will become a comprehensive research platform with DEMO-relevant technology in the field of fusion energy. It can also be a useful facility for spin-off of fusion technology for industrial applications. Along with CFETR engineering design and EAST experiments, the CRAFT will provide a solid technical base for successful construction of CFETR in the future. There are two main systems in the CRAFT. One is the superconducting magnet research system, and the other is the divertor research system.

Superconducting magnet research system

There are two parts in superconducting magnet research system. One is the conductor testing sub-system, and the other is the magnet testing sub-system (Figures 9A and 9B).

The function of the conductor testing sub-system is to test the large-scale CICCs used for the CFETR and the future DEMO. The maximum back field will reach 15 T, and the maximum current will reach 100 kA. It can perform DC, AC, and energy storage testing. The function of the magnet testing sub-system is to test TF and CS coils with large dimensions, such as the CFETR TF coil with dimensions of 23 × 20 m.

Divertor research system

The divertor is a critical component of the CFETR and DEMO. The operation conditions of the divertor are crucial; therefore, the divertor prototype and a testing facility should be developed to verify its performance, including its heat load handling capability, hydraulic performance, and material lifetime. A large linear plasma testing facility (Figure 9C) was designed' it could be operated steadily for 1,000 s with particle fluxes higher than 10^{24} m^{-2} s^{-1} and a magnetic field of 3 T. In this linear plasma testing facility, the plasma-facing materials and related components can be tested under realistic conditions, similar to those of the CFETR and DEMO.

Another important task for divertor research system construction is to achieve steady-state plasma discharge near the core. Therefore, plasma heating system must be developed, including an NBI system, an ECRH system, an LHCD system and an ICRF system. In addition, an RH and a 1/8 VV platform are planned to be developed, which will be integrated into the RH performance simulation device, as shown in Figure 9D.

The CRAFT is a national science facility aiming to develop key technologies and systems for the CFETR. The technologies created during the ITER project can be used; however, several key technologies need to be developed, and significant effort is needed. This will establish the method and standards for manufacturing key materials, components, and systems, alongside building key system prototypes for the CFETR. It is also fully open to the fusion research community, and additional construction and integrated experiments are encouraged.

PROSPECT

Nuclear fusion energy is a promising energy source that can solve energy shortage and environmental pollution issues. ASIPP built the EAST 15 years ago, and as the world's first fully superconducting tokamak, it has significantly advanced fusion research, including 100-s H-mode operation and 411-s long-pulse operation. Over the past few years, the EAST has been upgraded with an ITER-like active water-cooling tungsten divertor and is capable of handling a power load up to 10 MW/m^2 for long-pulse steady-state operation with high power injection. The EAST is a good platform for long-pulse and high-performance plasma investigations, and exploring ITER- and CFETR-related physics and engineering issues. China will continue to contribute to ITER construction by completing current CNDA procurements and will actively seek new contracts in the future. The ITER is still an experimental machine and suffers from several critical engineering issues relevant to future commercial fusion power plants; therefore, China is planning to build the CFETR to bridge the gaps between the ITER and DEMO. The primary goals of the CFETR project are to demonstrate a fusion energy production of 200–1000 MW and generate steady-state burning plasma with a duty time of about 50%. Currently, the engineering design of the CFETR has been completed, and several R&D activities are ongoing. To better understand the key technologies involved in the CFETR and future power plants, the construction of CRAFT platforms commenced in 2019 and will be finished in a few years.

REFERENCES

1. Huang, C., and Li, L. (2018). Magnetic confinement fusion: a brief review. Front. Energy Res. ***12***, 305–313.
2. Li, J., and Wan, Y. (2019). Present state of Chinese magnetic fusion development and future plans. J. Fusion Energy ***38***, 113–124.
3. Clery, D. (2019). Alternatives to tokamaks: a faster-better-cheaper route to fusion energy? Philos. Trans. R. Soc. A ***377***, 20170431.
4. Xu, Y. (2016). A general comparison between tokamak and stellarator plasmas. Matter Radiat. Extremes ***1***, 192–200.
5. Ye-xi, H. (2002). A research program of spherical tokamak in China. Plasma Sci. Technol. ***4***, 1355–1360.
6. Li, G., Li, L., and Xie, J. (1990). Characteristics of Low-Q Discharge on HT-6B Tokamak (China Nuclear Science and Technology Report), pp. 719–726.
7. Li, J., Luo, J., Wan, B., et al. (2000). Quasi-steady-state high confinement at high density by lower hybrid waves in the HT-6M tokamak. Nucl. Fusion ***40***, 467–471.
8. Yu, T., Qibing, H., Yong, L., et al. (1995). Simulation studies for lower hybrid current drive experiments on HL-1 tokamak (China Nuclear Science and Technology Report), pp. 11–12.
9. Liu, Y., Wang, E., Ding, X., et al. (2002). Overview of the HL-1M tokamak experiments. Fusion Sci. Technol. ***42***, 94–101.
10. Duan, X., Dong, J., Yan, L., et al. (2010). Preliminary results of ELMy H-mode experiments on the HL-2A tokamak. Nucl. Fusion ***50***, 095011.
11. Zheng, G., Xu, X., Ryutov, D., et al. (2014). Magnetic configuration flexibility of snowflake divertor for HL-2M. Fusion Eng. Des. ***89***, 2621–2627.
12. Zhuang, G., Pan, Y., Hu, X., et al. (2011). The reconstruction and research progress of the TEXT-U tokamak in China. Nucl. Fusion ***51***, 094020.
13. Zheng, J., Song, Y., Liu, X., et al. (2018). Overview of the design status of the superconducting magnet system of the CFETR. IEEE Trans. Appl. Supercond. ***28***, 1–5.
14. Minucci, S., Panella, S., Ciattaglia, S., et al. (2020). Electrical loads and power systems for the DEMO nuclear fusion project. Energies ***13***, 2269.
15. Okano, K., Kasada, R., Ikebe, Y., et al. (2018). An action plan of Japan toward development of demo reactor. Fusion Eng. Des. ***136***, 183–189.
16. Xu, G., Wan, B., Li, J., et al. (2011). Study on H-mode access at low density with lower hybrid current drive and lithium-wall coatings on the EAST superconducting tokamak. Nucl. Fusion ***51***, 072001.
17. Wan, B., and Collaborators, I. (2009). Recent experiments in the EAST and HT-7 superconducting tokamaks. Nucl. Fusion ***49***, 104011.
18. Guo, H., Li, J., Gong, X., et al. (2013). Approaches towards long-pulse divertor operations on EAST by active control of plasma–wall interactions. Nucl. Fusion ***54***, 013002.
19. Petrie, T., Fenstermacher, M., Holcomb, C., et al. (2017). Results from core-edge experiments in high Power, high performance plasmas on DIII-D. Nucl. Mater. Energy ***12***, 1141–1145.
20. Zhou, Z., Yao, D., and Cao, L. (2015). The upgrade of EAST divertor. J. Fusion Energy ***34***, 93–98.
21. Wan, B., Liang, Y., Gong, X., et al. (2019). Recent advances in EAST physics experiments in support of steady-state operation for ITER and CFETR. Nucl. Fusion ***59***, 112003.
22. Zang, Q., Zhao, J., Yang, L., et al. (2011). Upgraded multipulse laser and multipoint Thomson scattering diagnostics on EAST. Rev. Sci. Instrum. ***82***, 063502.
23. Zang, Q., Wang, T., Liang, Y., et al. (2016). Characteristics of edge pedestals in LHW and NBI heated H-mode plasmas on EAST. Nucl. Fusion ***56***, 106003.

24. Shi, Y., Wang, F., Wan, B., et al. (2010). Imaging x-ray crystal spectrometer on EAST. Plasma Phys. Control. Fusion ***52***, 085014.
25. Su, J., Wan, B., Huang, J., et al. (2021). Reconstructions of velocity distributions from fast-ion D-alpha (FIDA) measurements on EAST. Plasma Sci. Technol. ***23***, 095103.
26. Wang, Y., Hu, G., Xu, G., et al. (2019). Measurement of edge electron density profile with lithium beam emission spectroscopy (Li-BES) diagnostic on the experimental advanced superconducting tokamak (EAST). Fusion Eng. Des. ***144***, 133–140.
27. Huang, Y., Xiao, B., Luo, Z., et al. (2017). Development of real-time plasma current profile reconstruction with POINT diagnostic for EAST plasma control. Fusion Eng. Des. ***120***, 1–8.
28. Rasmussen, J.J., Nielsen, A.H., Madsen, J., et al. (2015). Numerical modeling of the transition from low to high confinement in magnetically confined plasma. Plasma Phys. Control. Fusion ***58***, 014031.
29. Li, J., Guo, H.Y., Wan, B.N., et al. (2013). A long-pulse high-confinement plasma regime in the Experimental Advanced Superconducting Tokamak. Nat. Phys. ***9***, 817–821.
30. Wan, B., Liang, Y., Gong, X., et al. (2017). Overview of EAST experiments on the development of high-performance steady-state scenario. Nucl. Fusion ***57***, 102019.
31. Gong, X., Wan, B., Li, J., et al. (2017). Realization of minute-long steady-state H-mode discharges on EAST. Plasma Sci. Technol. ***19***, 032001.
32. Wan, B., Li, J., Guo, H., et al. (2013). Progress of long pulse and H-mode experiments in EAST. Nucl. Fusion ***53***, 104006.
33. Wan, B., Li, J., Guo, H., et al. (2015). Advances in H-mode physics for long-pulse operation on EAST. Nucl. Fusion ***55***, 104015.
34. EAST 101-s discharge with a plasma temperature of 120 million °C. http://www.ipp.cas.cn/bm/dlztzd/kxyj/kyjz/202106/t20210610_643235.html.
35. Xu, L., Li, E., Zhou, T., et al. (2020). Observation of helical m/n = 1/1 saturated steady mode in EAST pure electron heating scenario with q0 $\leq$ 1. Nucl. Fusion ***60***, 106027.
36. Chinese "artificial sun" sets new world record. https://english.news.cn/20211231/c4fad387ef0745c18aedee05eed1414d/c.html.
37. Wagner, F. (2007). A quarter-century of H-mode studies. Plasma Phys. Control. Fusion ***49***, B1–B33.
38. Xu, G.S., Wan, B.N., Wang, H.Q., et al. (2011). First evidence of the role of zonal flows for theL—HTransition at marginal input power in the EAST tokamak. Phys. Rev. Lett. ***107***, 125001.
39. Xu, G., Wan, B., Wang, H., et al. (2016). Low-to-high confinement transition mediated by turbulence radial wave number spectral shift in a fusion plasma. Phys. Rev. Lett. ***116***, 095002.
40. Kirk, A., Wilson, H.R., Counsell, G.F., et al. (2004). Spatial and temporal structure of edge-localized modes. Phys. Rev. Lett. ***92***, 245002.
41. Sun, Y., Jia, M., Zang, Q., et al. (2016). Edge localized mode control using n= 1 resonant magnetic perturbation in the EAST tokamak. Nucl. Fusion ***57***, 036007.
42. Li, C., Hu, J., Chen, Y., et al. (2014). First results of pellet injection experiments on EAST. Plasma Sci. Technol. ***16***, 913–918.
43. Hu, J., Sun, Z., Li, C., et al. (2015). ELM mitigation by means of supersonic molecular beam and pellet injection on the EAST superconducting tokamak. J. Nucl. Mater. ***463***, 718–722.
44. Rack, M., Zeng, L., Denner, P., et al. (2014). Modelling of LHW-induced helical current filaments on EAST: study of an alternative method of applying RMPs. Nucl. Fusion ***54***, 064016.
45. Sun, Z., Qian, Y., Maingi, R., et al. (2021). Type-I ELM mitigation by continuous lithium granule gravitational injection into the upper tungsten divertor in EAST. Nucl. Fusion ***61***, 066022.
46. Sun, Y., Liang, Y., Liu, Y., et al. (2016). Nonlinear transition from mitigation to suppression of the edge localized mode with resonant magnetic perturbations in the EAST tokamak. Phys. Rev. Lett. ***117***, 115001.
47. Liang, Y., Gong, X.Z., Gan, K.F., et al. (2013). Magnetic topology changes induced by lower hybrid waves and their profound effect on edge-localized modes in the EAST tokamak. Phys. Rev. Lett. ***110***, 235002.
48. Hu, J., Sun, Z., Guo, H., et al. (2015). New steady-state quiescent high-confinement plasma in an experimental advanced superconducting tokamak. Phys. Rev. Lett. ***114***, 055001.
49. Xu, G.S., Yang, Q.Q., Yan, N., et al. (2019). Promising high-confinement regime for steady-state fusion. Phys. Rev. Lett. ***122***, 255001.
50. Kong, D., Xu, X., Diamond, P., et al. (2018). E× B flow shear mitigates ballooning-driven edge-localized modes at high collisionality: experiment and simulation. Nucl. Fusion ***59***, 016016.
51. Gong, X., Garofalo, A.M., Huang, J., et al. (2019). Integrated operation of steady-state long-pulse H-mode in experimental advanced superconducting tokamak. Nucl. Fusion ***59***, 086030.
52. Wu, K., Yuan, Q.P., Xiao, B.J., et al. (2018). Achievement of radiative feedback control for long-pulse operation on EAST. Nucl. Fusion ***58***, 056019.
53. Liu, J.B., Wang, L., Guo, H.Y., et al. (2019). Divertor detachment and asymmetry in H-mode operation with an ITER-like tungsten divertor in EAST. Nucl. Fusion ***59***, 126046.
54. Meng, L.Y., Liu, J.B., Xu, J.C., et al. (2020). Experimental study of detachment density threshold in L-mode plasmas on EAST. Plasma Phys. Control. Fusion ***62***, 065008.
55. Liu, X.J., Deng, G.Z., Wang, L., et al. (2017). Modeling study of radiation characteristics with different impurity species seeding in EAST. Phys. Plasmas ***24***, 122509.
56. Wang, L., Wang, H.Q., Ding, S., et al. (2021). Integration of full divertor detachment with improved core confinement for tokamak fusion plasmas. Nat. Commun. ***12***, 1365.
57. Wang, L., Xu, G.S., Hu, J.S., et al. (2021). Progress of divertor heat and particle flux control in EAST for advanced steady-state operation in the last 10 years. J. Fusion Energy ***40***, 3.
58. Wang, L., Guo, H., Ding, F., et al. (2019). Advances in plasma–wall interaction control for H-mode operation over 100 s with ITER-like tungsten divertor on EAST. Nucl. Fusion ***59***, 086036.
59. Bigot, B. (2019). Progress toward ITER's first plasma. Nucl. Fusion ***59***, 112001.
60. Campbell, D. (2016). The first fusion reactor: ITER. EuroPhys. News ***47***, 28–31.
61. Bigot, B. (2019). ITER construction and manufacturing progress toward first plasma. Fusion Eng. Des. ***146***, 124–129.
62. ITER website. https://www.iter.org.
63. Breschi, M., Devred, A., Casali, M., et al. (2012). Results of the TF conductor performance qualification samples for the ITER project. Supercond. Sci. Technol. ***25***, 095004.
64. Song, Y., Bauer, P., Bi, Y., et al. (2010). Design of the ITER TF magnet feeder systems. IEEE Trans. Appl. Supercond. ***20***, 1710–1713.
65. Huang, S., Gao, G., Fu, P., et al. (2019). Design, manufacturing, acceptance testing and quality control of ITER PF AC/DC converters. Fusion Eng. Des. ***138***, 59–67.
66. Chen, J., Liu, X., Wang, P., et al. (2019). Progress in developing ITER and DEMO first wall technologies at SWIP. Nucl. Fusion ***60***, 016005.
67. Leng, Z., Chen, J., Wang, K., et al. (2020). Hot helium leak test of ITER blanket shield block. Fusion Eng. Des. ***153***, 111498.
68. Federici, G., Bachmann, C., Biel, W., et al. (2016). Overview of the design approach and prioritization of R&D activities towards an EU DEMO. Fusion Eng. Des. ***109–111***, 1464–1474.
69. Tobita, K., Hiwatari, R., Utoh, H., et al. (2018). Overview of the DEMO conceptual design activity in Japan. Fusion Eng. Des. ***136***, 1024–1031.
70. Zhuang, G., Li, G., Li, J., et al. (2019). Progress of the CFETR design. Nucl. Fusion ***59***, 112010.
71. Chan, V., Stambaugh, R.D., Stambaugh, R., et al. (2010). Physics basis of a fusion development facility utilizing the tokamak approach. Fusion Sci. Technol. ***57***, 66–93.
72. Kovari, M., Kemp, R., Lux, H., et al. (2014). PROCESS": a systems code for fusion power plants—Part 1: Physics. Fusion Eng. Des. ***89***, 3054–3069.
73. Morris, J., Chan, V., Chen, J., et al. (2019). Validation and sensitivity of CFETR design using EU systems codes. Fusion Eng. Des. ***146***, 574–577.
74. Li, H., Li, G.Q., Liu, X.J., et al. (2020). Optimization design for plasma configuration at the CFETR. Fusion Eng. Des. ***152***, 111447.
75. Liu, X.J., Xu, G.L., Ding, R., et al. (2020). Simulation studies of divertor power exhaust with Neon seeding for CFETR with GW-level fusion power. Phys. Plasmas ***27***, 092508.
76. Meneghini, O., Snyder, P.B., Smith, S.P., et al. (2016). Integrated fusion simulation with self-consistent core-pedestal coupling. Phys. Plasmas ***23***, 042507.
77. Snyder, P.B., Groebner, R.J., Leonard, A.W., et al. (2009). Development and validation of a predictive model for the pedestal height. Phys. Plasmas ***16***, 056118.
78. Staebler, G.M., Kinsey, J.E., and Waltz, R.E. (2005). Gyro-Landau fluid equations for trapped and passing particles. Phys. Plasmas ***12***, 102508.
79. Kernbichler, W., Kasilov, S.V., Leitold, G.O., et al. (2008). Recent progress in NEO-2 — A code for neoclassical transport computations based on field line tracing. Plasma Fusion Res. ***3***, S1061.
80. Chen, J., Chan, V.S., Jian, X., et al. (2021). Integrated modeling of CFETR hybrid scenario plasmas. Nucl. Fusion ***61***, 046002.
81. Li, Z.Y., Zhu, Y.R., Xu, G.L., et al. (2021). Edge localized mode characteristics and divertor heat flux during stationary and transient phase for CFETR hybrid scenario. Plasma Phys. Control. Fusion ***63***, 035006.
82. Stankiewicz, R., and Zagórski, R. (2005). Influence of core–edge coupling and impurities on the operation regimes of a fusion reactor. J. Nucl. Mater. ***337–339***, 191–195.
83. Xie, H., Chan, V.S., Ding, R., et al. (2020). Evaluation of tritium burnup fraction for CFETR scenarios with core-edge coupling simulations. Nucl. Fusion ***60***, 046022.
84. Qian, J.P., Garofalo, A.M., Gong, X.Z., et al. (2021). Advances in physics understanding of high poloidal beta regime toward steady-state operation of CFETR. Phys. Plasmas ***28***, 042506.
85. Song, Y.T., Wu, S.T., Li, J.G., et al. (2014). Concept design of CFETR tokamak machine. IEEE Trans. Plasma Sci. ***42***, 503–509.

ACKNOWLEDGMENTS

The author would like to express gratitude to all individuals who made contributions to the projects of EAST, ITER CNDA procurement packages, CFETR, and CRAFT. This work is supported by the National Key R&D Program of China under contract 2017YFE0300500 and the Comprehensive Research Facility for Fusion Technology Program of China under contract 2018-000052-73-01-001228.

AUTHOR CONTRIBUTIONS

J.Z., J.Q., Q.Z., Z.L., L.W., R.D., J.C., P.L., L.X., and L.C. wrote the draft manuscript. G.X., J.H., and X.G. critically revised the manuscript. K.L., M.X., X.D., and Y.S. performed supervision and project administration. All authors reviewed and provided revisions for the manuscript.

DECLARATION OF INTERESTS

The authors declare no competing interests.

LEAD CONTACT WEBSITE

http://ferd.ipp.ac.cn/display.php?id=311.